

Analysis of Three-Dimensional Sediment Gravity Flows

Amiruddin*, Shinji SASSA**, Hideo SEKIGUCHI

* Graduate School of Engineering, Kyoto University

** Port and Airport Research Institute, 1-1 Nagase, Yokosuka

Synopsis

A three-dimensional analysis procedure for describing the behaviour of liquefied soil with a free surface has been developed in the present study. The liquefied soil is modelled as a heavy, incompressible viscous fluid. A set of three-dimensional Navier-Stokes equations and the continuity equation are numerically solved under moving boundary conditions. For the purpose of identifying the moving interface between the ambient fluid and the liquefied soil, the volume-of-fluid technique (Hirt and Nicholas, 1981) is adopted. The predictive capability of the proposed analysis procedure is discussed with reference to a class of dam-break problems in which a column of water in air collapses under its own weight. The predicted performance compares favourably with results of two-dimensional experiments of Martin and Moyce (1952), encouraging further test of the three-dimensional analysis code developed.

Keywords: dam-break problem, gravity current, liquefied soil, three-dimensional analysis

1. Introduction

In recent years, offshore pipeline engineering has increasingly dealt with continental slopes and deep waters. This means new problems have to be faced, which were previously disregarded. Among these, the hazard of sediment gravity flows has received attention due to the richness in the physics involved and environmental consequences (Hampton et. al, 1996; Simpson, 1997). Sediment gravity flows are essentially downslope currents of material denser than the ambient water. They include subaqueous debris flows and turbidity currents (Drago, 2002).

The importance of pore water pressures in the dynamics of debris flows was pointed out by Iverson (1997). The developments of pore water pressures may exert significant effects on the process of subaqueous liquefied sediment flow as well. Sassa et al. (2003)

developed a two-dimensional analysis code named LIQSEDFLOW by combining a set of two-dimensional Navier-Stokes equations for a fully liquefied soil domain with a consolidation equation for a solidifying soil domain.

The aim of this study is to extend LIQSEDFLOW so as to deal with truly three-dimensional nature of liquefied sediment flows. Toward this goal this paper restricts the discussion into a fluid-dynamics module only. The fluid-dynamics module is based on a set of three-dimensional Navier-Stokes equations for a fully liquefied soil domain that are to be combined with consolidation equations for a solidifying soil domain. The Navier-Stokes equations together with the equation of continuity may be solved using a finite difference method. Specifically, a simplified MAC method (Amsden and Harlow, 1970) in terms of staggered rectilinear grid is applied, and the Poisson equations

regarding the excess pore pressures may be solved using the conjugate gradient (CG) method (Ferziger and Peric, 1997). For tracking the moving interface between the ambient fluid and the liquefied soil, we will adopt the volume-of-fluid (VOF) technique (Hirt and Nichols, 1981). An efficient volume-advection scheme (Hamzah, 2001) will also be used to ensure the conservation of mass in the course of the liquefied flow.

We will then examine the validity of the proposed analysis procedure against a class dam-break problems, in which a column of water in air collapses under its own weight.

2. The Numerical Model Developed

2.1 The governing equations

Consider a body of liquefied soil underwater. One of the simplest yet meaningful modeling for the liquefied soil is to regard it as a heavy, incompressible viscous fluid with a free surface. There follow

$$\frac{\partial u}{\partial x} + \frac{\partial v}{\partial y} + \frac{\partial w}{\partial z} = 0 \quad (1)$$

$$\frac{\partial u}{\partial t} + u \frac{\partial u}{\partial x} + v \frac{\partial u}{\partial y} + w \frac{\partial u}{\partial z} = g_x - \frac{1}{\rho} \frac{\partial p}{\partial x} + \nu \left(\frac{\partial^2 u}{\partial x^2} + \frac{\partial^2 u}{\partial y^2} + \frac{\partial^2 u}{\partial z^2} \right) \quad (2a)$$

$$\frac{\partial v}{\partial t} + u \frac{\partial v}{\partial x} + v \frac{\partial v}{\partial y} + w \frac{\partial v}{\partial z} = g_y - \frac{1}{\rho} \frac{\partial p}{\partial y} + \nu \left(\frac{\partial^2 v}{\partial x^2} + \frac{\partial^2 v}{\partial y^2} + \frac{\partial^2 v}{\partial z^2} \right) \quad (2b)$$

$$\frac{\partial w}{\partial t} + u \frac{\partial w}{\partial x} + v \frac{\partial w}{\partial y} + w \frac{\partial w}{\partial z} = g_z - \frac{1}{\rho} \frac{\partial p}{\partial z} + \nu \left(\frac{\partial^2 w}{\partial x^2} + \frac{\partial^2 w}{\partial y^2} + \frac{\partial^2 w}{\partial z^2} \right) \quad (2c)$$

where u , v and w are the velocity in x , y and z directions, respectively; ρ is the fluid density, g_x , g_y and g_z are the components of gravitational acceleration, p is the pressure, ν is the kinematic viscosity.

2.2 Boundary conditions

Let Ω be a fluid domain, bounded by Σ , inside which consider a material surface moving with the fluid whose equation is $F(\vec{x}, t) = 0$ (Fig. 1). The material surface $F(\vec{x}, t) = 0$ may be called a free surface or an interface when it represents a surface across which the properties of the medium are discontinuous.

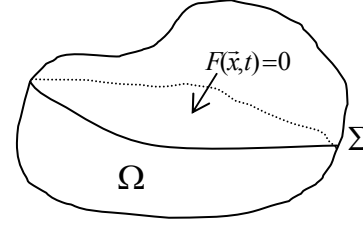


Fig. 1 Solution domain for fluid flow problem

(1) Boundary conditions on Σ

On Σ , one or more components of fluid velocity \vec{u} can be prescribed, i.e.

$$\vec{u}(\vec{x}, t) = \vec{w}(\vec{x}, t) \quad \vec{x} \in \Sigma; \quad t \geq 0 \quad (3)$$

$$\int_{\Sigma} \vec{w} \cdot \vec{n} dS = 0 \quad t \geq 0 \quad (4)$$

In Eqs. (3) - (4), \vec{w} is the prescribed velocity on Σ . The last of these equations results from applying the divergence theorem to the continuity equation and sets an integral constraint on the normal component of the velocity on Σ . It is also possible to specify Neumann-type boundary conditions on velocity, which are conditions for the normal and/or tangential components of the stress. These boundary conditions take the form

$$\sigma_n = (\vec{\sigma} \cdot \vec{n}) \cdot \vec{n} \quad \vec{x} \in \Sigma; \quad t \geq 0 \quad (5a)$$

$$\sigma_t = (\vec{\sigma} \cdot \vec{n}) \cdot \vec{t} \quad \vec{x} \in \Sigma; \quad t \geq 0 \quad (5b)$$

If the flow is two-dimensional and the boundary has small curvature, the two stress conditions can be written as

$$\sigma_n = -p + 2\mu \frac{\partial u_n}{\partial n}; \quad u_n = \vec{u} \cdot \vec{n} \quad (6a)$$

$$\sigma_t = \mu \left(\frac{\partial u_n}{\partial t} + \frac{\partial u_t}{\partial n} \right); \quad u_t = \vec{u} \cdot \vec{t} \quad (6b)$$

In three dimensions, there are two local, linearly independent, tangential directions. Provided boundary conditions are always prescribed for each velocity component at any boundary point, both Dirichlet or Neumann conditions can be chosen, in either normal or tangential directions. It is also possible to specify different types of boundary conditions on different parts of Σ .

An important case with stress conditions are free-slip condition, in which the tangential stress is set to zero. This boundary condition is not appropriate for real

viscous fluids, but it is useful in the numerical approximations to the Navier-Stokes equations when the effect of viscosity is relatively small and the boundary layers near the walls cannot be resolved (Lemos, 1994).

(2) Free-surface boundary conditions

A free-surface is a material surface across which the density is assumed to be discontinuous. A material surface always consists of the same particles. The rate at which any function varies for a moving particle is given the material derivative of F . Thus the kinematical relation defining a surface moving with the fluid is

$$\frac{DF}{Dt} = \frac{\partial F}{\partial t} + \vec{u} \cdot \nabla F = 0 \quad (7)$$

Conversely, by requiring the motion to be continuous, it can be shown that a surface satisfying this equation always consists of the same particles. Fixed or moving walls also satisfy this equation, but in general Eq. (7) should be regarded as another equation to be solved if the position of the material surface F cannot be known *a-priori*.

The existence of a free surface poses three problems. The first is how to determine of its position. The second is how to determine of its time evolution. The third is the prescription of the correct boundary conditions on all points of the free surface. Since these boundary conditions depend on the location and shape of the free surface, the three problems are interrelated.

At a material surface, two transition relationships must be satisfied. One is the continuity of velocity. The other is the continuity of stress vector. The continuity of velocity is a purely kinematical constraint and is called the kinematic boundary condition. It is mathematically expressed by Eq. (7). The continuity of the stress vector is also required to prevent the material surface from acquiring an infinite acceleration and is called the dynamic boundary condition. The continuity of the tangential component of the stress vector is expressed by the following equality

$$\mu \left(\frac{\partial u_i}{\partial x_j} + \frac{\partial u_j}{\partial x_i} \right) n_i t_j \Big|_{\text{med1}} = \mu \left(\frac{\partial u_i}{\partial x_j} + \frac{\partial u_j}{\partial x_i} \right) n_i t_j \Big|_{\text{med2}} \quad (8)$$

In three-dimensional problems this equation must be satisfied along different directions defined linearly independent vectors \vec{t} that lie on the local tangent plane to F . In two-dimensional problems, Eq. (8) becomes a

scalar equation.

The continuity of the component of the stress vector, gives the following equation

$$p - \mu \left(\frac{\partial u_i}{\partial x_j} + \frac{\partial u_j}{\partial x_i} \right) n_i n_j \Big|_{\text{med1}} = p - \mu \left(\frac{\partial u_i}{\partial x_j} + \frac{\partial u_j}{\partial x_i} \right) n_i n_j + p_s \Big|_{\text{med2}} \quad (9)$$

where p_s is the surface tension pressure. Surface tension is important in capillary waves, which sustain wind stress in the sea, and the combination of surface tension and air entrainment originates much of the complexity of aerated regions in breaking flow. Such effects are too complex to be included in the present formulation. Therefore, for the purposes of this work, surface tension is neglected.

If the free surface separates fluids of very different densities, the dynamic free-surface boundary conditions can be simplified. This is the case in fluid-gas interface, in which the density and viscosity of the gas are much smaller than those of the fluid. Consequently, the pressure variations in the gas are much smaller if the velocities and their derivatives have comparable magnitude. Thus, the following approximate equations may be used

$$\mu \left(\frac{\partial u_i}{\partial x_j} + \frac{\partial u_j}{\partial x_i} \right) n_i t_j = 0 \quad (10)$$

$$p - \mu \left(\frac{\partial u_i}{\partial x_j} + \frac{\partial u_j}{\partial x_i} \right) n_i n_j = p_0 \quad (11)$$

These equations are tangential and normal stress conditions, respectively. The left-hand sides of Eqs. (10) and (11) refer to conditions in the fluid, whereas the right-hand sides refer to conditions in the gas. If the fluid is treated as an ideal fluid, the normal stress condition is $p = p_0$. This is called the inviscid free-surface boundary condition.

2.3 Numerical method

(1) Computational mesh and internal obstacles

(a) Computational mesh

The governing equations (1) - (2) are discretized in a non-uniform Eulerian mesh by using the MAC finite

difference method (Amsden and Harlow, 1970). The x -, y - and z -momentum transports are respectively calculated at the right, back and top faces of a cell and the continuity equation is calculated at the center of the cell (Fig. 2(a)). The computational domain is surrounded by a layer of fictitious cells. These cells are used to set velocity boundary conditions so that the same discretized equations are used in the whole computational domain.

(b) Internal obstacles

Internal obstacles may be introduced as a special case of two-phase flow in such a way that the first phase represents the fluid with a volume fraction Θ and the second phase represents obstacle with a volume fraction equal to $1.0 - \Theta$ (Kothe et al., 1994). The obstacle is characterized as a fluid of infinite density and has zero velocity. The volume fraction Θ is assumed to take zero in the obstacle material and take one in the fluid. The partial flow flag Θ becomes a perfect step function only when obstacle boundaries coincide with mesh lines that represent lines of constant x , y and z .

In general, obstacle boundaries can arbitrarily snake through the mesh, cutting through cells. This gives rise to Θ values in the range $(0.0 \leq \Theta \leq 1.0)$, which is necessary to avoid a stair-step model of a curved interior obstacle boundary. Those cells having values of Θ satisfying $(0.0 \leq \Theta \leq 1.0)$ are termed partial flow cells. This is because a volumetric portion Θ of such a cell is open to flow while the remaining portion $(1.0 - \Theta)$ is occupied by an obstacle that impedes to flow.

Refer to Fig. 2(b) for the partial cell treatment with internal obstacles (shaded region). In the presence of internal obstacles, the finite difference equations are facilitated by defining for each partial cell a volume fraction $\Theta_{i,j,k}$ at the cell center, an area fraction $\Theta_{i+1/2,j,k}$ at the right face, an area fraction $\Theta_{i,j+1/2,k}$ at the front face, and an area fraction $\Theta_{i,j,k+1/2}$ at the top face.

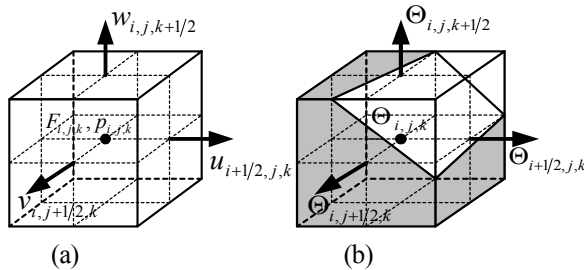


Fig. 2 The 3-D staggered mesh arrangement
(a) Layout of dependent variables
(b) Partial cell treatment for internal obstacles

(2) Procedure of computation

The computational procedure proceeds as follows (Fig. 3). Use explicit approximations to the Navier–Stokes equations to compute the first guess for new-time-level velocities. To satisfy the continuity equation, perform pressure–velocity iterations. This procedure is a variant of Newton’s method and is applied to the Poisson equation with respect to pressure in incompressible flow. More specifically, pressures are iteratively adjusted in each cell and velocity changes induced by the pressure changes are added to the velocities that have been computed using the Navier–Stokes equations with the predetermined pressure field. The function F , defining fluid-occupied regions, is updated to give the new fluid configuration. All mesh cells are reflagged as full cells, surface cells or empty cells. All variables are updated, the time and cycle counters are incremented and the computational cycle is restarted.

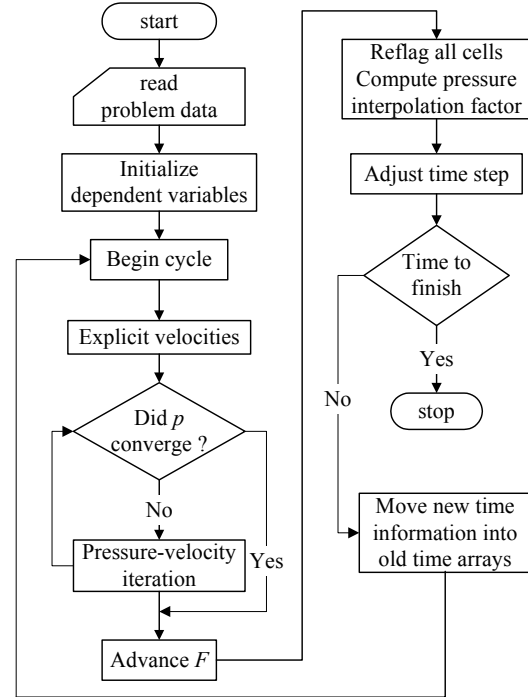


Fig. 3 Flowchart of the computer program

(3) Finite-difference approximations to momentum conservation equations

A standard finite-difference approximation to Eqs. (2) in MAC-type methods is expressed as

$$u_{i+1/2,j,k}^{n+1} = u_{i+1/2,j,k}^n + \frac{\Delta t}{\rho} \left(\frac{\partial p}{\partial x} \right)^{n+1} + \Delta t (-FUX - FUY - FUZ + g_x + VISX)^n \quad (12a)$$

$$v_{i,j+1/2,k}^{n+1} = v_{i,j+1/2,k}^n + \frac{\Delta t}{\rho} \left(\frac{\partial p}{\partial y} \right)^{n+1} + \Delta t (-FVX - FVY - FVZ + g_y + VISY)^n \quad (12b)$$

$$w_{i,j,k+1/2}^{n+1} = w_{i,j,k+1/2}^n + \frac{\Delta t}{\rho} \left(\frac{\partial p}{\partial z} \right)^{n+1} + \Delta t (-FWX - FWY - FWZ + g_z + VISZ)^n \quad (12c)$$

Following Hirt and Nichols (1981), the convective terms in Eqs. (12) are discretized using a combination of first-order donor-cell and centered-difference approximations. The expression for FUX is then given by

$$FUX = \frac{u_{i+1/2,j,k}^n}{\Delta x_{\alpha}} [\Delta x_{i+1} DUL + \Delta x_i DUR] + \alpha \operatorname{sgn}(u_{i+1/2,j,k}^n) (\Delta x_{i+1} DUL - \Delta x_i DUR) \quad (13a)$$

where

$$\begin{aligned} DUR &= (u_{i+3/2,j,k}^n - u_{i+1/2,j,k}^n) / \Delta x_{i+1} \\ DUL &= (u_{i+1/2,j,k}^n - u_{i-1/2,j,k}^n) / \Delta x_i \\ \Delta x_{\alpha} &= \Delta x_i + \Delta x_{i+1} + \alpha \operatorname{sgn}(u_{i+1/2,j,k}^n) (\Delta x_{i+1} - \Delta x_i) \end{aligned}$$

When $\alpha = 0$, expression (13a) reduces to the second-order accurate centered-difference approximation. For $\alpha = 1$, the first-order donor-cell form is recovered. The expressions for FUY and FUZ are given by

$$FUY = \frac{v_{i+1/2,j,k}^n}{\Delta y_{\alpha}} [\Delta y_{j+1/2} DUB + \Delta y_{j-1/2} DUF] + \alpha \operatorname{sgn}(v_{i+1/2,j,k}^n) (\Delta y_{j+1/2} DUB - \Delta y_{j-1/2} DUF) \quad (13b)$$

$$FUZ = \frac{w_{i+1/2,j,k}^n}{\Delta z_{\alpha}} [\Delta z_{k+1/2} DUA + \Delta z_{k-1/2} DUT] + \alpha \operatorname{sgn}(w_{i+1/2,j,k}^n) (\Delta z_{k+1/2} DUA - \Delta z_{k-1/2} DUT) \quad (13c)$$

where

$$\begin{aligned} DUF &= (u_{i+1/2,j+1,k}^n - u_{i+1/2,j,k}^n) / \Delta y_{j+1/2} \\ DUB &= (u_{i+1/2,j,k}^n - u_{i+1/2,j-1,k}^n) / \Delta y_{j-1/2} \\ DUT &= (u_{i+1/2,j,k+1}^n - u_{i+1/2,j,k}^n) / \Delta z_{k+1/2} \\ DUA &= (u_{i+1/2,j,k}^n - u_{i+1/2,j,k-1}^n) / \Delta z_{k-1/2} \\ \Delta y_{\alpha} &= \Delta y_{j+1/2} + \Delta y_{j-1/2} + \alpha \operatorname{sgn}(v_{i+1/2,j,k}^n) (\Delta y_{j+1/2} - \Delta y_{j-1/2}) \\ \Delta z_{\alpha} &= \Delta z_{k+1/2} + \Delta z_{k-1/2} + \alpha \operatorname{sgn}(w_{i+1/2,j,k}^n) (\Delta z_{k+1/2} - \Delta z_{k-1/2}) \end{aligned}$$

Likewise, the approximations for the convective accelerations in the y -direction are:

$$FVX = \frac{u_{i,j+1/2,k}^n}{\Delta x_{\alpha y}} [\Delta x_{i+1/2} DVL + \Delta x_{i-1/2} DVR] + \alpha \operatorname{sgn}(u_{i,j+1/2,k}^n) (\Delta x_{i+1/2} DVL - \Delta x_{i-1/2} DVR) \quad (14a)$$

$$FVY = \frac{v_{i,j+1/2,k}^n}{\Delta y_{\alpha y}} [\Delta y_{j+1} DVB + \Delta y_j DVF] + \alpha \operatorname{sgn}(v_{i,j+1/2,k}^n) (\Delta y_{j+1} DVB - \Delta y_j DVF) \quad (14b)$$

$$FVZ = \frac{w_{i,j+1/2,k}^n}{\Delta z_{\alpha y}} [\Delta z_{k+1/2} DUA + \Delta z_{k-1/2} DUT] + \alpha \operatorname{sgn}(w_{i,j+1/2,k}^n) (\Delta z_{k+1/2} DUA - \Delta z_{k-1/2} DUT) \quad (14c)$$

where

$$\begin{aligned} DVR &= (v_{i+1,j+1/2,k}^n - v_{i,j+1/2,k}^n) / \Delta x_{i+1/2} \\ DVL &= (v_{i,j+1/2,k}^n - v_{i-1,j+1/2,k}^n) / \Delta x_{i-1/2} \\ DVF &= (v_{i,j+3/2,k}^n - v_{i,j+1/2,k}^n) / \Delta y_{j+1} \\ DVB &= (v_{i,j+1/2,k}^n - v_{i,j-1/2,k}^n) / \Delta y_j \\ DVT &= (v_{i,j+1/2,k+1}^n - v_{i,j+1/2,k}^n) / \Delta z_{k+1/2} \\ DVA &= (v_{i,j+1/2,k}^n - v_{i,j+1/2,k-1}^n) / \Delta z_{k-1/2} \\ \Delta x_{\alpha y} &= \Delta x_{i+1/2} + \Delta x_{i-1/2} + \alpha \operatorname{sgn}(u_{i,j+1/2,k}^n) (\Delta x_{i+1/2} - \Delta x_{i-1/2}) \\ \Delta y_{\alpha y} &= \Delta y_{j+1} + \Delta y_j + \alpha \operatorname{sgn}(v_{i,j+1/2,k}^n) (\Delta y_{j+1} - \Delta y_j) \\ \Delta z_{\alpha y} &= \Delta z_{k+1/2} + \Delta z_{k-1/2} + \alpha \operatorname{sgn}(w_{i,j+1/2,k}^n) (\Delta z_{k+1/2} - \Delta z_{k-1/2}) \end{aligned}$$

The approximations for the convective accelerations in the z -direction read:

$$FWX = \frac{u_{i,j,k+1/2}^n}{\Delta x_{\alpha z}} [\Delta x_{i+1/2} DWL + \Delta x_{i-1/2} DWR] + \alpha \operatorname{sgn}(u_{i,j,k+1/2}^n) (\Delta x_{i+1/2} DWL - \Delta x_{i-1/2} DWR) \quad (15a)$$

$$FWY = \frac{v_{i,j,k+1/2}^n}{\Delta y_{\alpha z}} [\Delta y_{j+1/2} DWB + \Delta y_{j-1/2} DWF] + \alpha \operatorname{sgn}(v_{i,j,k+1/2}^n) (\Delta y_{j+1/2} DWB - \Delta y_{j-1/2} DWF) \quad (15b)$$

$$FWZ = \frac{w_{i,j,k+1/2}^n}{\Delta z_{\alpha z}} [\Delta z_{k+1} DWA + \Delta z_k DWT] + \alpha \operatorname{sgn}(w_{i,j,k+1/2}^n) (\Delta z_{k+1} DWA - \Delta z_k DWT) \quad (15c)$$

where

$$\begin{aligned} DWR &= (w_{i+1,j,k+1/2}^n - w_{i,j,k+1/2}^n) / \Delta x_{i+1/2} \\ DWL &= (w_{i,j,k+1/2}^n - w_{i-1,j,k+1/2}^n) / \Delta x_{i-1/2} \end{aligned}$$

$$\begin{aligned}
DWF &= (w_{i,j+1,k+1/2}^n - v_{i,j,k+1/2}^n) / \Delta y_{j+1/2} \\
DWB &= (w_{i,j,k+1/2}^n - v_{i,j-1,k+1/2}^n) / \Delta y_{j-1/2} \\
DWT &= (w_{i,j,k+3/2}^n - w_{i,j,k+1/2}^n) / \Delta z_{k+1} \\
DWA &= (w_{i,j,k+1/2}^n - w_{i,j,k-1/2}^n) / \Delta z_k \\
\Delta x_{\alpha z} &= \Delta x_{i+1/2} + \Delta x_{i-1/2} + \alpha \operatorname{sgn}(u_{i,j,k+1/2}^n) \\
&\quad \times (\Delta x_{i+1/2} - \Delta x_{i-1/2}) \\
\Delta y_{\alpha z} &= \Delta y_{j+1/2} + \Delta y_{j-1/2} + \alpha \operatorname{sgn}(v_{i,j,k+1/2}^n) \\
&\quad \times (\Delta y_{j+1/2} - \Delta y_{j-1/2}) \\
\Delta z_{\alpha z} &= \Delta z_{k+1} + \Delta z_k + \alpha \operatorname{sgn}(w_{i,j,k+1/2}^n) (\Delta z_{k+1} - \Delta z_k)
\end{aligned}$$

Here $\Delta x_{i+1/2} = (\Delta x_{i+1} + \Delta x_i) / 2$, $\Delta y_{j+1/2} = (\Delta y_{j+1} + \Delta y_j) / 2$ and $\Delta z_{k+1/2} = (\Delta z_{k+1} + \Delta z_k) / 2$. When the quantities in the finite-difference expressions are required at positions where they are not defined (e.g. $v_{i+1/2,j,k}^n$ in *FUY* $u_{i,j+1/2,k}^n$ in *FVX*, etc), they are interpolated before using them in the finite-difference equations. When a product between any quantities is required, the quantities are averaged (interpolated) before the product is formed.

Lemos (1994) reduced a finite-difference to a differential equation by expanding each of the finite difference-function terms in a Taylor series. The lowest order terms in the expansion represent the original differential equation being approximated. All higher order terms constitute the truncation errors caused by the finite-difference approximation. The stability of a finite-difference equation can often be determined from an examination of these truncation errors. If only diffusion truncation errors are retained to order Δt and Δx^2 , the finite-difference equations (12) can be reduced to

$$\begin{aligned}
\frac{\partial u}{\partial t} + u \frac{\partial u}{\partial x} + v \frac{\partial u}{\partial y} + w \frac{\partial u}{\partial z} &= -\frac{1}{\rho} \frac{\partial p}{\partial x} + g_x \\
&+ \left(v - \frac{\Delta t}{2} u^2 - \frac{\Delta x^2}{2} \frac{\partial u}{\partial x} \right) \frac{\partial^2 u}{\partial x^2} + \left(v - \frac{\Delta t}{2} v^2 \right. \\
&\quad \left. - \frac{\Delta x^2}{2} \frac{\partial v}{\partial y} \right) \frac{\partial^2 u}{\partial y^2} + \left(v - \frac{\Delta t}{2} w^2 - \frac{\Delta z^2}{2} \frac{\partial w}{\partial z} \right) \frac{\partial^2 u}{\partial z^2}
\end{aligned} \quad (16a)$$

$$\begin{aligned}
\frac{\partial v}{\partial t} + u \frac{\partial v}{\partial x} + v \frac{\partial v}{\partial y} + w \frac{\partial v}{\partial z} &= -\frac{1}{\rho} \frac{\partial p}{\partial y} + g_y \\
&+ \left(v - \frac{\Delta t}{2} u^2 - \frac{\Delta x^2}{2} \frac{\partial u}{\partial x} \right) \frac{\partial^2 v}{\partial x^2} + \left(v - \frac{\Delta t}{2} v^2 \right. \\
&\quad \left. - \frac{\Delta x^2}{2} \frac{\partial v}{\partial y} \right) \frac{\partial^2 v}{\partial y^2} + \left(v - \frac{\Delta t}{2} w^2 - \frac{\Delta z^2}{2} \frac{\partial w}{\partial z} \right) \frac{\partial^2 v}{\partial z^2}
\end{aligned} \quad (16b)$$

$$\begin{aligned}
\frac{\partial w}{\partial t} + u \frac{\partial w}{\partial x} + v \frac{\partial w}{\partial y} + w \frac{\partial w}{\partial z} &= -\frac{1}{\rho} \frac{\partial p}{\partial z} + g_z \\
&+ \left(v - \frac{\Delta t}{2} u^2 - \frac{\Delta x^2}{2} \frac{\partial u}{\partial x} \right) \frac{\partial^2 w}{\partial x^2} + \left(v - \frac{\Delta t}{2} v^2 \right. \\
&\quad \left. - \frac{\Delta x^2}{2} \frac{\partial v}{\partial y} \right) \frac{\partial^2 w}{\partial y^2} + \left(v - \frac{\Delta t}{2} w^2 - \frac{\Delta z^2}{2} \frac{\partial w}{\partial z} \right) \frac{\partial^2 w}{\partial z^2}
\end{aligned} \quad (16c)$$

In comparing Eqs. (16) with Eqs. (2), we find additional terms in Eqs. (16). Those terms involving Δt result from the first-order approximation to $\partial u / \partial t$, $\partial v / \partial t$ and $\partial w / \partial t$, while terms containing Δx^2 , Δy^2 or Δz^2 stem from evaluating undefined variables by simple average formulas and from computing derivatives of u^2 , v^2 , w^2 , uv , uw and vw terms. These additional terms represent negative diffusion coefficients so that the finite-difference scheme might yield growing unstable solutions if the viscosity ν is smaller than the truncation errors terms. Thus, according to Lemos (1994), the following discretization of the viscous term in Eqs. (12) was adopted:

$$\begin{aligned}
VISX &= \left[\nu + (1 - \alpha) \frac{\Delta t}{2} (u_{i+1/2,j,k}^n)^2 \right] \left[\frac{DUR - DUL}{\Delta x_{i+1/2}} \right] \\
&+ \left[\nu + (1 - \alpha) \frac{\Delta t}{2} (u_{i+1/2,j,k}^n)^2 \right] \left[\frac{DUF - DUB}{\Delta y_j} \right] \\
&+ \left[\nu + (1 - \alpha) \frac{\Delta t}{2} (u_{i+1/2,j,k}^n)^2 \right] \left[\frac{DUT - DUA}{\Delta z_k} \right]
\end{aligned} \quad (17a)$$

$$\begin{aligned}
VISY &= \left[\nu + (1 - \alpha) \frac{\Delta t}{2} (v_{i,j+1/2,k}^n)^2 \right] \left[\frac{DVR - DVL}{\Delta x_i} \right] \\
&+ \left[\nu + (1 - \alpha) \frac{\Delta t}{2} (v_{i,j+1/2,k}^n)^2 \right] \left[\frac{DVF - DVB}{\Delta y_{j+1/2}} \right] \\
&+ \left[\nu + (1 - \alpha) \frac{\Delta t}{2} (v_{i,j+1/2,k}^n)^2 \right] \left[\frac{DVT - DVA}{\Delta z_k} \right]
\end{aligned} \quad (17b)$$

$$\begin{aligned}
VISZ &= \left[\nu + (1 - \alpha) \frac{\Delta t}{2} (w_{i,j,k+1/2}^n)^2 \right] \left[\frac{DWR - DWL}{\Delta x_i} \right] \\
&+ \left[\nu + (1 - \alpha) \frac{\Delta t}{2} (w_{i,j,k+1/2}^n)^2 \right] \left[\frac{DWF - DWB}{\Delta y_j} \right] \\
&+ \left[\nu + (1 - \alpha) \frac{\Delta t}{2} (w_{i,j,k+1/2}^n)^2 \right] \left[\frac{DWT - DWA}{\Delta z_{k+1/2}} \right]
\end{aligned} \quad (17c)$$

(4) Finite-difference approximations to continuity equation

Velocities computed from Eqs. (12) in general will not satisfy the continuity equation because p^{n+1} is not available. To satisfy the continuity equation and to determine the correct pressure, values of pressures and velocities must be adjusted in each cell that is occupied by fluid. In a full cell, pressure is changed in such a way that the divergence D_{ijk} left by the first step is driven to zero; in a free-surface cell, the cell pressure may be determined in such a way that a linear interpolation between the pressure in the surface and adjacent full cell yields the wanted value p_s (usually zero) at the

free-surface location. In both cases, the velocities located on the sides of the cell are simultaneously adjusted, in response to the pressure change in the cell.

The pressure in a full cell is split into an old time-level component and a correction such that

$$\Delta p_{i,j,k} \equiv P_{i,j,k}^{n+1} - P_{i,j,k}^n \quad (18)$$

Then we can work out the pressure derivatives:

$$\left(\frac{\partial p}{\partial x}\right)^{n+1} = \frac{\partial}{\partial x}(p^{n+1} - p^n + p^n) = \frac{\partial \Delta p}{\partial x} + \left(\frac{\partial p}{\partial x}\right)^n$$

$$\left(\frac{\partial p}{\partial y}\right)^{n+1} = \frac{\partial}{\partial y}(p^{n+1} - p^n + p^n) = \frac{\partial \Delta p}{\partial y} + \left(\frac{\partial p}{\partial y}\right)^n$$

$$\left(\frac{\partial p}{\partial z}\right)^{n+1} = \frac{\partial}{\partial z}(p^{n+1} - p^n + p^n) = \frac{\partial \Delta p}{\partial z} + \left(\frac{\partial p}{\partial z}\right)^n$$

Substituting these in the momentum equations gives:

$$u_{i+1/2,j,k}^{n+1} = u_{i+1/2,j,k}^n + \frac{\Delta t}{\rho} \frac{\partial \Delta p}{\partial x} + \Delta t \left(\frac{1}{\rho} \frac{\partial p}{\partial x} - FUX - FUY - FUZ + g_x + VISX \right)^n \quad (19a)$$

$$v_{i,j+1/2,k}^{n+1} = v_{i,j+1/2,k}^n + \frac{\Delta t}{\rho} \frac{\partial \Delta p}{\partial y} + \Delta t \left(\frac{1}{\rho} \frac{\partial p}{\partial y} - FVX - FVY - FVZ + g_y + VISY \right)^n \quad (19b)$$

$$w_{i,j,k+1/2}^{n+1} = w_{i,j,k+1/2}^n + \frac{\Delta t}{\rho} \frac{\partial \Delta p}{\partial z} + \Delta t \left(\frac{1}{\rho} \frac{\partial p}{\partial z} - FWX - FWY - FWZ + g_z + VISZ \right)^n \quad (19c)$$

Let us define the following quantities:

$$D^n \equiv \left[\frac{\partial u}{\partial x} + \frac{\partial v}{\partial y} + \frac{\partial w}{\partial z} \right]^n$$

$$Q_x^n = \left[\frac{1}{\rho} \frac{\partial p}{\partial x} - FUX - FUY - FUZ + g_x + VISX \right]^n$$

$$Q_y^n = \left[\frac{1}{\rho} \frac{\partial p}{\partial y} - FVX - FVY - FVZ + g_y + VISY \right]^n$$

$$Q_z^n = \left[\frac{1}{\rho} \frac{\partial p}{\partial z} - FWX - FWY - FWZ + g_z + VISZ \right]^n$$

Then the momentum equations are written as:

$$u_{i+1/2,j,k}^{n+1} = u_{i+1/2,j,k}^n - \frac{\Delta t}{\rho} \frac{\partial \Delta p}{\partial x} + Q_x^n \quad (20a)$$

$$v_{i,j+1/2,k}^{n+1} = v_{i,j+1/2,k}^n - \frac{\Delta t}{\rho} \frac{\partial \Delta p}{\partial y} + Q_y^n \quad (20b)$$

$$w_{i,j,k+1/2}^{n+1} = w_{i,j,k+1/2}^n - \frac{\Delta t}{\rho} \frac{\partial \Delta p}{\partial z} + Q_z^n \quad (20c)$$

The iterative method starts with calculating a first estimate of the velocities with a fully explicit guess ($\Delta p^{(1)} = 0$):

$$u_{i+1/2,j,k}^{(1)} = u_{i+1/2,j,k}^n + Q_x^n \quad (21a)$$

$$v_{i,j+1/2,k}^{(1)} = v_{i,j+1/2,k}^n + Q_y^n \quad (21b)$$

$$w_{i,j,k+1/2}^{(1)} = w_{i,j,k+1/2}^n + Q_z^n \quad (21c)$$

For an improved guess the pressure correction $\Delta p^{(2)}$ should be included such that

$$u_{i+1/2,j,k}^{(2)} = u_{i+1/2,j,k}^{(1)} - \frac{\Delta t}{\rho} \left(\frac{\partial \Delta p}{\partial x} \right)^{(2)} \quad (22a)$$

$$v_{i,j+1/2,k}^{(2)} = v_{i,j+1/2,k}^{(1)} - \frac{\Delta t}{\rho} \left(\frac{\partial \Delta p}{\partial y} \right)^{(2)} \quad (22b)$$

$$w_{i,j,k+1/2}^{(2)} = w_{i,j,k+1/2}^{(1)} - \frac{\Delta t}{\rho} \left(\frac{\partial \Delta p}{\partial z} \right)^{(2)} \quad (22c)$$

Substitute these into the continuity equation. Then, a form of Poisson equation results:

$$\nabla^2(\Delta p)^{(2)} = \frac{\rho D^{(1)}}{\Delta t} \quad (23)$$

This equation can be solved for $\Delta p^{(2)}$. For this purpose we used finite differences taking into consideration the variable mesh to obtain:

$$D_{i,j,k}^{(1)} = \frac{\Delta t}{\rho} \left[\frac{1}{\Delta x_i} \left(\frac{\Delta p_{i+1,j,k}^{(2)} - \Delta p_{i,j,k}^{(2)}}{\Delta x_{i+1/2,j,k}} - \frac{\Delta p_{i,j,k}^{(2)} - \Delta p_{i-1,j,k}^{(2)}}{\Delta x_{i-1/2,j,k}} \right) + \frac{1}{\Delta y_j} \left(\frac{\Delta p_{i,j+1,k}^{(2)} - \Delta p_{i,j,k}^{(2)}}{\Delta y_{i,j+1/2,k}} - \frac{\Delta p_{i,j,k}^{(2)} - \Delta p_{i,j-1,k}^{(2)}}{\Delta y_{i,j-1/2,k}} \right) + \frac{1}{\Delta z_k} \left(\frac{\Delta p_{i,j,k+1}^{(2)} - \Delta p_{i,j,k}^{(2)}}{\Delta z_{i,j,k+1/2}} - \frac{\Delta p_{i,j,k}^{(2)} - \Delta p_{i,j,k-1}^{(2)}}{\Delta z_{i,j,k-1/2}} \right) \right]$$

The pressure correction $\Delta p^{(2)}$ is now computed from the requirement $D_{i,j,k}^{(2)} = 0$ such that

$$\Delta p_{i,j,k}^{(2)} = -\frac{S}{(\partial S / \partial p)} \quad (24)$$

with

$$S = D_{i,j,k}^{(1)} \equiv \frac{\Theta_{i+1/2,j,k} u_{i+1/2,j,k}^{(1)} - \Theta_{i-1/2,j,k} u_{i-1/2,j,k}^{(1)}}{\Theta_{i,j,k} \Delta x_i} + \frac{\Theta_{i,j+1/2,k} v_{i,j+1/2,k}^{(1)} - \Theta_{i,j-1/2,k} v_{i,j-1/2,k}^{(1)}}{\Theta_{i,j,k} \Delta y_j} + \frac{\Theta_{i,j,k+1/2} w_{i,j,k+1/2}^{(1)} - \Theta_{i,j,k-1/2} w_{i,j,k-1/2}^{(1)}}{\Theta_{i,j,k} \Delta z_k}$$

$$\frac{\partial S}{\partial p} = \frac{\Delta t}{\rho \Theta_{i,j,k}} \left[\frac{1}{\Delta x_i} \left(\frac{\Theta_{i+1/2,j,k}}{\Delta x_{i+1/2}} + \frac{\Theta_{i-1/2,j,k}}{\Delta x_{i-1/2}} \right) + \frac{1}{\Delta y_j} \left(\frac{\Theta_{i,j+1/2,k}}{\Delta y_{j+1/2}} + \frac{\Theta_{i,j-1/2,k}}{\Delta y_{j-1/2}} \right) + \frac{1}{\Delta z_k} \left(\frac{\Theta_{i,j,k+1/2}}{\Delta z_{k+1/2}} + \frac{\Theta_{i,j,k-1/2}}{\Delta z_{k-1/2}} \right) \right]$$

Convergence of Eq. (24), which is a variant of the Newton-Raphson relaxation technique, can be accelerated if $D_{i,j,k}^{(1)}$ is multiplied by an over-relaxation factor ω such that $1 \leq \omega \leq 2$. An optimum value of ω is often equal to 1.7; an unstable iteration results if ω exceeds 2 (Hirt and Cook, 1972).

In order to deal with a free surface, we need an additional procedure because the location of the free surface is unknown *a priori*. The procedure adopted herein is described in brief as follows (refer to Fig. 4). The surface cell pressure $p_{i,j,k}$ may be determined by a linear interpolation (or extrapolation) between the surface pressure, p_s , and pressure, p_N , inside the fluid. Namely,

$$p_{i,j,k}^{n+1} = (1-\zeta)p_N + \zeta p_s \quad (25)$$

where $\zeta = d_c/d$ is the ratio of the distance between the cell centers to the distance between the free surface and the center of the neighbor interpolation cell. When the surface tension effect is neglected, p_s can be set zero. Equation (24) can be used to compute the pressure correction for a surface cell, provided S is replaced by

$$S = (1-\zeta)p_N + \zeta p_s - p_{i,j,k} \quad (26)$$

After the pressure correction is found from Eq. (24), neighbor velocities are updated using Eq. (22). The pressure correction is always computed using the most up-to-date velocities.

$$p_{i,j,k}^{(2)} = p_{i,j,k}^{(n)} + \Delta p_{i,j,k}^{(2)} \quad (27)$$

$$u_{i\pm 1/2,j,k}^{(2)} = u_{i\pm 1/2,j,k}^{(1)} \pm \frac{\Delta t}{\rho \Delta x_{i\pm 1/2,j,k}} \Delta p_{i,j,k}^{(2)} \quad (28a)$$

$$v_{i,j\pm 1/2,k}^{(2)} = v_{i,j\pm 1/2,k}^{(1)} \pm \frac{\Delta t}{\rho \Delta y_{j\pm 1/2,k}} \Delta p_{i,j,k}^{(2)} \quad (28b)$$

$$w_{i,j,k\pm 1/2}^{(2)} = w_{i,j,k\pm 1/2}^{(1)} \pm \frac{\Delta t}{\rho \Delta z_{k\pm 1/2}} \Delta p_{i,j,k}^{(2)} \quad (28c)$$

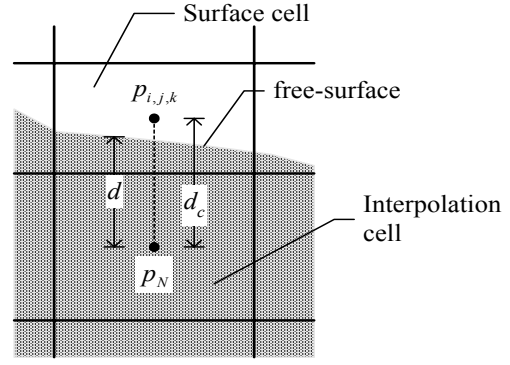


Fig. 4 Sketch for pressure interpolation procedure

In summary, the procedure of pressure iteration can be stated as follows (refer to Fig 5). The correction of pressure is calculated from either Eq. (24) for full cells or from Eq. (26) for free surface cells. The corrected pressure is then obtained from Eq. (27). The velocities compatible with the new corrected pressure are obtained from Eqs. (28). This process is done iteratively until the $D_{i,j,k}^{(n)}$ term becomes sufficiently small such that the velocity field is in required accuracy.

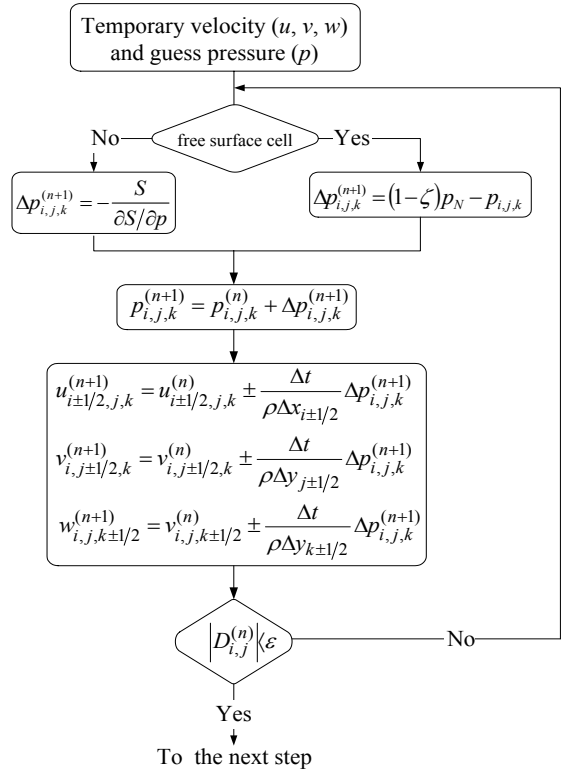


Fig. 5 Flowchart of pressure-velocity iteration

(5) Numerical treatment of free surfaces

A free surface poses three problems in numerical fluid dynamics: the surface must be numerically described; the surface must be advanced in time; and

appropriate boundary conditions must be applied at the location of the surface. These three problems are interrelated, because the algorithm used to advance the free surface in time depends on the method used to define the free surface, and the boundary conditions can only be applied after the location and shape of the surface are known.

(a) Free-surface representation methods

The main issue is that free-surface representation methods should be able to treat any free surface configuration (nearly horizontal, nearly vertical, bubbles, drops, overturning surfaces, etc) economically and without logical problems. Two types of such methods have been used for defining the location and shape of free surfaces: line/interface methods and region (or volume) methods. Examples of the first type are the height function and line segment methods. Examples of region methods are the use of marker particles and those with “volume of fluid” techniques.

Height functions are the simplest method for treating free surface problems. The free surface is defined by a distance from a reference line. Thus, for a free surface that is nearly horizontal, the reference line may be the bottom of the mesh and $\eta = \eta(x, t)$, the height above that datum, may be approximated by a set of discrete values of η . In this approach, the slope of the surface $\partial\eta/\partial x$ must be smaller than the mesh aspect ratio $\Delta y/\Delta x$. Furthermore, the method does not work at all with multiple surfaces.

Line segments are a generalization of the height-function method. In this method, the free surface is defined as a chain of short segments. These segments are defined by sets of ordered points whose coordinates are stored. The length of such a segment should be smaller than the minimum cell size. More storage is required than in the previous case, but the method is not limited to single-valued surfaces. There is one important difficulty, however. When surfaces intersect or when a surface fold over itself, segment chains must be reordered. Detection of such intersections and efficient reordering are difficult if not impossible.

Thus, the methods which define fluid regions rather than interfaces are advantageous in situations involving multiple free boundaries. This eliminates all ordering problems found in line/surface methods.

The first of the region methods may be the marker-and-cell (MAC) method. Storage requirements

with this method increase significantly, because a large number of particle coordinates must be stored. It is also time consuming to move all marker particles (an average of four to ten marker particles per cell is needed). A free surface is defined as a cell that contains marker particles and has at least one neighbour cell without marker particles. The actual location of the free-surface position within the cell is determined by an additional computation based on the distribution of marker particles within the cell.

Marker particle methods offer the distinct advantage of eliminating all logic problems associated with intersecting surfaces. This is primarily a consequence of the fact that while particles have to be ordered when marking regions. The particle method is also readily extendable to three-dimensional computations, provided the increased storage requirements can be tolerated.

In retrospect, it appears that a method that defines fluid regions rather than interfaces offers the advantage of logical simplicity for situations involving intersecting multiple free-surface boundaries. While the marker particle method provides this simplicity, it suffers from a significant increase in required computer storage. It also requires additional computational time to move all the points to new locations. It is natural, therefore, to seek an alternative that shares the region defining property without an excessive use of computer resources. Such a method is described in the next section.

(b) Volume-of-fluid (VOF) method

In the VOF method, a free surface is represented on the fixed grids using fractional fluid volume in a cell (or in a control volume). Each rectangle in Fig. 6 denotes a unit cell. The fractional volume of fluid, F , is defined such that it is equal to unity at any point occupied by fluid and zero otherwise (Hirt and Nichols, 1981). As the free surface moves, the fractional volume-of-fluid of each cell is updated. In a numerical sense, every cell is classified into three categories according to the value of F (see Fig. 6). If a cell is completely filled with fluid, the fractional volume-of-fluid of the cell is unity ($F = 1$) and the cell is considered to be in the main flow region. If a cell is empty ($F = 0$), it belongs to an empty region and its contribution to the computation of the flow field is excluded. A cell is considered to be on the free surface when the value of F lies between 0 and 1 ($0 < F < 1$).

Although the VOF technique can locate free boundaries nearly as well as a distribution of marker

particles, and with a minimum of stored information, the method is worthless unless an algorithm can be devised for accurately computing the evaluation of the F filled. The time dependence of F is governed by Eq. (7). The fact that F is a step function with values of zero or one permits the use of a flux approximation that preserves its discontinuous nature. This approximation, referred to as the donor-acceptor scheme (Hirt and Nichols, 1981), is described in more detail in the next section.

In summary, the VOF method offers a region-following scheme with minimum storage requirements. Furthermore, because it follows regions rather than surfaces, all logic problems associated with intersecting surfaces are avoided with the VOF technique. The method is also applicable to three-dimensional computations, where its conservative use of stored information is highly advantageous.

Thus, the VOF method provides a simple and economical way to track free surface boundaries in two- or three-dimensional meshes. In principle, the method could be used to track surfaces of discontinuity in material properties, in tangential velocity, or any other property. The particular case being represented determines the specific boundary condition that must be applied at the location of the boundary. For situations where the surface does not remain fixed in the fluid, but has some additional relative motion, the equation of motion, Eq. (7), should be modified.

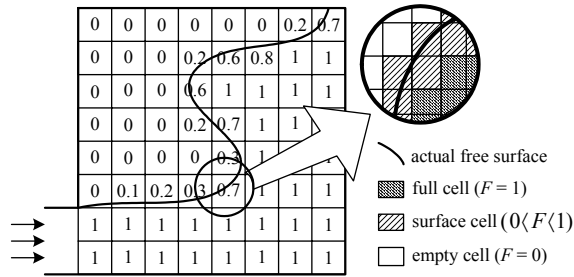


Fig. 6 Numerical methods for volume-of-fluid method

(c) Methods for updating a free surface

The kinematic condition for the advection of the VOF function (Eq. 7) can be written in finite difference form as:

$$F_{i,j,k}^{n+1} = F_{i,j,k}^n - \Delta t \left(u \frac{\partial F}{\partial x} + v \frac{\partial F}{\partial y} + w \frac{\partial F}{\partial z} \right) \quad (29)$$

The convective terms may be rearranged to divergence form, minus a divergence correction term:

$$u \frac{\partial F}{\partial x} + v \frac{\partial F}{\partial y} + w \frac{\partial F}{\partial z} = \frac{\partial(Fu)}{\partial x} + \frac{\partial(Fv)}{\partial y} + \frac{\partial(Fw)}{\partial z} - F \left(\frac{\partial u}{\partial x} + \frac{\partial v}{\partial y} + \frac{\partial w}{\partial z} \right) \quad (30)$$

Substituting (30) into (29) we get the divergence part:

$$\hat{F}_{i,j,k} = F_{i,j,k}^n - \Delta t \left[\frac{\partial(Fu)}{\partial x} + \frac{\partial(Fv)}{\partial y} + \frac{\partial(Fw)}{\partial z} \right]^n \quad (31)$$

which is then updated with the correction:

$$F_{i,j,k}^{n+1} = \hat{F}_{i,j,k} - \Delta t F_{i,j,k}^n \left(\frac{\partial u}{\partial x} + \frac{\partial v}{\partial y} + \frac{\partial w}{\partial z} \right)^{n+1} \quad (32)$$

This sequence insures conservative advection of F (Kothe et al., 1994). Ordinarily, the correction in (32) would be zero due to continuity. However, it has been found desirable to include the correction numerically because although the magnitude is small yet non-zero and of the order of $\varepsilon \Delta t$.

The divergence equation for F can be finite differenced for the advection term in the x -direction in terms of an upstream donor (d) cell at (id, j, k) and a downstream acceptor (a) cell at (ia, j, k) (if $u_{i,j,k}^{n+1} > 0$, $idm = i - 1$, $id = i$, $ia = i + 1$, otherwise, $ia = i$, $id = i + 1$, $idm = i + 2$):

$$\begin{aligned} \hat{F}_{id,j,k} &= F_{id,j,k}^n - \frac{\Delta t \Delta(Fu)}{\Delta x_{id}} \\ \hat{F}_{ia,j,k} &= F_{ia,j,k}^n + \frac{\Delta t \Delta(Fu)}{\Delta x_{ia}} \end{aligned} \quad (33)$$

Here the amount of F fluxed across the cell face in Δt is:

$$\Delta t \Delta(Fu) = \min \left(F_{iad,j,k} |u_{i+1/2,j,k}^{n+1} \Delta t| + CF_x, F_{id,j,k} \Delta x_{id} \right) \quad (34)$$

with the correction factor:

$$CF_x = \max \left[\left(F_{idm,j,k} - F_{iad,j,k} \right) u_{i+1/2,j,k}^{n+1} \Delta t - \left(F_{idm,j,k} - F_{id,j,k} \right) \Delta x_{id}, 0 \right] \quad (35)$$

In these expressions, superscript a denotes the acceptor cell, subscript d denotes the donor cell, and double subscript ad corresponds to either a or d depending on the surface orientation. Double subscript dm denotes the upstream of the donor cell and Δx_{id} stands for the width of the donor cell. The operator \min in Eq. (34) prevents

the fluxing of more F from the donor cell than it has to give, while the operator \max in Eq. (35) accounts for an additional F flux, CF_x , if the amount of void $(1-F)$ to be fluxed exceeds the amount of void available in the donor cell. Fig. 7 provides a pictorial explanation of Eq. (34), where the shaded region represents the amount of fluid in each cell and the striped region represents the amount of fluid to be fluxed. The donor and acceptor cells are defined in Fig. 7a for fluxing across a vertical cell face.

Following Nichols and Hirt (1981), the rules for choosing $ad = a$ or $ad = d$ are the following. When $ad = d$, the flux is an ordinary donor-cell value, $F = F_d|V|$, in which the F value in the donor cell is used to define the fractional area of the cell face fluxing, as shown in Fig. 7b. When $ad = a$, the value of F in the acceptor cell is used to define the fractional area of the cell face across which fluid is flowing. In case (c) of Fig. 7, all the fluid in the donor cell is fluxed because everything lying between the dashed line and the flux boundary moves into the acceptor cell. In case (d) of Fig. 7, more fluid than the amount $F = F_a|V|$, must be fluxed, the extra fluid between the dashed line and the flux boundary is equal to the CF_x value in Eq. (34).

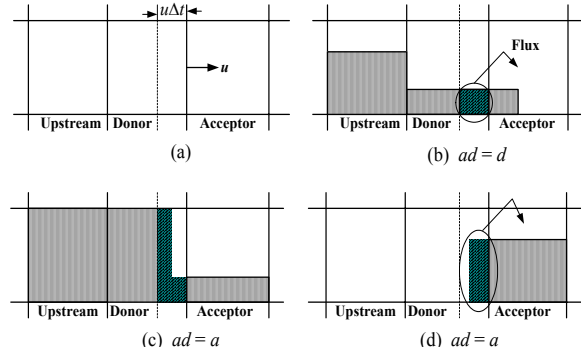


Fig. 7 Examples of free-surface shapes used in the advection of F

Likewise, the approximations for F -convection in y -direction can be expressed as:

$$\begin{aligned}\hat{F}_{i,jd,k} &= F_{i,jd,k}^n - \frac{\Delta t \Delta(Fv)}{\Delta y_{jd}} \\ \hat{F}_{i,ja,k} &= F_{i,ja,k}^n + \frac{\Delta t \Delta(Fv)}{\Delta y_{ja}}\end{aligned}\quad (36)$$

Here the amount of F fluxed across the cell face in Δt is:

$$\Delta t \Delta(Fv) = \min\left(F_{i,jad,k} \left|v_{i,j+1/2,k}^{n+1} \Delta t\right| + CF_y, F_{i,jd,k} \Delta y_{jd}\right) \quad (37)$$

with the correction factor:

$$CF_y = \max\left[\left(F_{i,jdm,k} - F_{i,jad,k}\right) v_{i,j+1/2,k}^{n+1} \Delta t \left| - \left(F_{i,jdm,k} - F_{i,jd,k}\right) \Delta y_{jd}, 0\right]\quad (38)$$

The F -convection in z -direction can be expressed as:

$$\begin{aligned}\hat{F}_{i,jkd} &= F_{i,jkd}^n - \frac{\Delta t \Delta(Fw)}{\Delta z_{kd}} \\ \hat{F}_{i,jka} &= F_{i,jka}^n + \frac{\Delta t \Delta(Fw)}{\Delta z_{ka}}\end{aligned}\quad (39)$$

Here the amount of F fluxed across the cell face in Δt is:

$$\Delta t \Delta(Fw) = \min\left(F_{i,jkad} \left|w_{i,j,k+1/2}^{n+1} \Delta t\right| + CF_z, F_{i,jkd} \Delta z_{kd}\right) \quad (40)$$

with the correction factor:

$$CF_z = \max\left[\left(F_{i,jkdm} - F_{i,jkad}\right) w_{i,j,k+1/2}^{n+1} \Delta t \left| - \left(F_{i,jkdm} - F_{i,jkd}\right) \Delta z_{kd}, 0\right]\quad (41)$$

Finally, the divergence correction is added:

$$F_{i,j,k}^{n+1} = \hat{F}_{i,j,k} + \Delta t F_{i,j,k}^n D_{i,j,k}^{n+1} \quad (42)$$

(d) Discretization of free-surface boundary conditions

After deciding which method will be used for free-surface representation and updating, it is necessary to impose the correct stress conditions at the free-surface location. For a three-dimensional surface, the normal and tangential stress conditions are

$$\begin{aligned}p - 2\mu \left[\frac{\partial u}{\partial x} n_x^2 + \frac{\partial v}{\partial y} n_y^2 + \frac{\partial w}{\partial z} n_z^2 \right. \\ \left. + \left(\frac{\partial u}{\partial y} + \frac{\partial v}{\partial x} \right) n_x n_y + \left(\frac{\partial u}{\partial z} + \frac{\partial w}{\partial x} \right) n_x n_z \right. \\ \left. + \left(\frac{\partial v}{\partial z} + \frac{\partial w}{\partial y} \right) n_y n_z \right] = 0\end{aligned}\quad (43)$$

$$\begin{aligned}\mu \left[2 \frac{\partial u}{\partial x} n_x t_{1x} + 2 \frac{\partial v}{\partial y} n_y t_{1y} + 2 \frac{\partial w}{\partial z} n_z t_{1z} \right. \\ \left. + \left(\frac{\partial u}{\partial y} + \frac{\partial v}{\partial x} \right) (n_x t_{1y} + n_y t_{1x}) \right. \\ \left. + \left(\frac{\partial u}{\partial z} + \frac{\partial w}{\partial x} \right) (n_x t_{1z} + n_z t_{1x}) \right. \\ \left. + \left(\frac{\partial v}{\partial z} + \frac{\partial w}{\partial y} \right) (n_y t_{1z} + n_z t_{1y}) \right] = 0\end{aligned}\quad (44a)$$

$$\begin{aligned}
& \mu \left[2 \frac{\partial u}{\partial x} n_x t_{2x} + 2 \frac{\partial v}{\partial y} n_y t_{2y} + 2 \frac{\partial w}{\partial z} n_z t_{2z} \right. \\
& \quad + \left(\frac{\partial u}{\partial y} + \frac{\partial v}{\partial x} \right) (n_x t_{2y} + n_y t_{2x}) \\
& \quad + \left(\frac{\partial u}{\partial z} + \frac{\partial w}{\partial x} \right) (n_x t_{2z} + n_z t_{2x}) \\
& \quad \left. + \left(\frac{\partial v}{\partial z} + \frac{\partial w}{\partial y} \right) (n_y t_{2z} + n_z t_{2y}) \right] = 0
\end{aligned} \tag{44b}$$

where n_x , n_y , and n_z are the components of the unit vector normal to the surface, and $t_{1x}, t_{1y}, t_{1z}, t_{2x}, t_{2y}, t_{2z}$ are components of the tangential unit vector. In these equations it is assumed that the influence of the gas on the fluid is negligible. For a free surface of small curvature these conditions can be replaced by the simpler expressions

$$p - 2\mu \frac{\partial u_n}{\partial n} = 0 \tag{45}$$

$$\mu \left(\frac{\partial u_n}{\partial t} + \frac{\partial u_t}{\partial n} \right) = 0 \tag{46}$$

Usually, these simplified stress conditions are used in place of completing stress conditions because the former is rigorous yet difficult to use (Nichols and Hirt, 1971).

The normal stress condition is imposed as a boundary condition for the pressure. Incorrect normal stress conditions result in a loss of momentum conservation in free-surface cells; the free surface may move too slowly or too fast, and the calculation may become unstable. The type of pressure boundary conditions in free surface codes (MAC and SMAC), consisted of simply setting $p_{i,j,k} = p_s$, regardless of the position of the surface within the cell. This technique was not very satisfactory, however. An improved method consists of determining the free-surface position within the cell (Nichols and Hirt, 1971). Then, the pressure on the center of the surface cell is set in such a way that an interpolation (or extrapolation) between the surface cell and the adjacent interpolation cell yields $p = p_s$ at the free surface (refer to Fig. 4) is given by Eq. (25)

The correct tangential stress condition is given by Eq. (46). To apply this condition, it is necessary to know the position and shape of the free surface. If the surface cell has only one neighboring empty cell, the boundary velocity is set to ensure the vanishing of the velocity divergence. When there are two or more empty neighbour cells, the individual contributions to the

divergence equation are separately set to zero. Suppose, for instance, that there are two adjacent surface cells (i, j, k) and $(i+1, j, k)$ in such a way that they have two adjacent empty cells $(i, j, k+1)$ and $(i+1, j, k+1)$ (see Fig. 8). Accordingly, tangential stress conditions may be imposed by setting the velocities at all boundaries between the surface and empty cells in terms of the discretized continuity equation for the surface cell. Namely,

$$\begin{aligned}
w_{i,j,k+1/2} = w_{i,j,k-1/2} - \Delta z_k \left[\left(\frac{u_{i+1/2,j,k} - u_{i-1/2,j,k}}{\Delta x_i} \right) \right. \\
\left. - \left(\frac{v_{i,j+1/2,k} - v_{i,j-1/2,k}}{\Delta y_j} \right) \right]
\end{aligned} \tag{47}$$

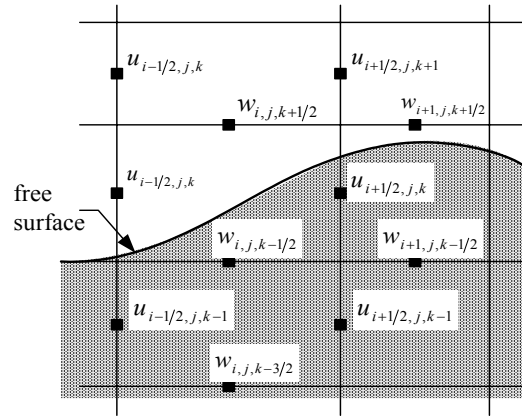


Fig. 8 Sketch for discretized tangential stress condition

(e) Fluid volume adjustments

The value ΔF computed using the above procedure is subtracted from the donor cell and added to the acceptor cell. This process is repeated for all cell boundaries in the mesh, and the resulting F values define the new fluid configuration. Occasionally, the time-advanced F values may become slightly less than zero, or slightly greater than unity. A remedy for these situations may be done as follows. After the F -convection calculation has been completed, the mesh is swept to reset values of F being less than zero back to zero, and values of F being greater than one back to one. Accumulated changes in fluid volume introduced by these adjustments during a calculation are recorded and may be printed out at any time.

There is another adjustment needed in F in order that it may be used as a surface cell flag. A surface cell has values of F lying between zero and one and at least one neighbouring cell that is empty. However, F values cannot be tested against exact numbers such as zero and

one because round off error would cause spurious results. Instead, a cell is defined to be empty when F is less than ε_F and to be full when F is greater than $(1 - \varepsilon_F)$. Here ε_F is typically 10^{-6} . If, after advection, a cell has an F value less than ε_F , this F is set to zero and all neighbouring full cells become surface cells by having their F values reduced from unity by an amount $1.1\varepsilon_F$. These changes in F are also included in the accumulated volume change. It is observed that typically volume errors after hundreds of cycles are only a fraction of one per cent of the total fluid volume.

(f) Determining interfaces within a cell

For the accurate application of the normal-stress boundary condition, it is necessary to determine the location of the free surface within the surface cell. In addition, it may be necessary to know the local free-surface curvature (e.g. if surface tension effects are to be included). In VOF technique, it is assumed that the boundary can be approximated by a straight line cutting through the cell. By first determining the slope of this line, it can be moved across the cell to a position that intersects the known amount of fluid volume in the cell.

For VOF slope calculation, a cell block is used in this study so that the slope between a surface cell and a neighboring cell does not lose its accuracy even though the neighbouring cell is empty. A cell block is constructed of a surface cell and its eight neighbouring cells as shown in Fig. 8. For calculating the slope at the face of a surface cell by use of neighbouring cells, it is assumed that the interface of the free surface can be represented by a single-valued function $f(x)$ or $f(y)$ in the x - or y -direction of the real computational domain. If the surface is represented as $f(x)$, $f(x)$ can be approximated as three cell columns that are the sum of the volume fraction from cell $(j-1)$ to cell $(j+1)$ for each cell column of Fig. 9:

$$f_{i-1} = \frac{\sum_{k=j-1}^{j+1} (\Delta y_k F_{i-1,k})}{H} \quad (48a)$$

$$f_i = \frac{\sum_{k=j-1}^{j+1} (\Delta y_k F_{i,k})}{H} \quad (48a)$$

$$f_{i+1} = \frac{\sum_{k=j-1}^{j+1} (\Delta y_k F_{i+1,k})}{H} \quad (48a)$$

where $H = \sum_{k=j-1}^{j+1} \Delta y_k$ and $f = 0$ are taken as the bottom edge of the $(j-1)$ row of the cells.

The average slope at the center of a cell block is calculated by equation (49)

$$\left(\frac{\partial f}{\partial x} \right)_{AVG} = \frac{\frac{f_{i+1} - f_i}{\Delta x_{i+1/2}} \Delta x_{i-1/2} + \frac{f_i - f_{i-1}}{\Delta x_{i-1/2}} \Delta x_{i+1/2}}{\Delta x_{i+1/2} + \Delta x_{i-1/2}} \quad (49)$$

A similar calculation can be made for $\partial f / \partial y$, i.e.

$$f_{j-1} = \frac{\sum_{k=i-1}^{i+1} (\Delta x_k F_{k,j-1})}{H} \quad (50a)$$

$$f_j = \frac{\sum_{k=i-1}^{i+1} (\Delta x_k F_{k,j})}{H} \quad (50b)$$

$$f_{j+1} = \frac{\sum_{k=i-1}^{i+1} (\Delta x_k F_{k,j+1})}{H} \quad (50c)$$

$$\left(\frac{\partial f}{\partial y} \right)_{AVG} = \frac{\frac{f_{j+1} - f_j}{\Delta y_{j+1/2}} \Delta y_{j-1/2} + \frac{f_j - f_{j-1}}{\Delta y_{j-1/2}} \Delta y_{j+1/2}}{\Delta y_{j+1/2} + \Delta y_{j-1/2}} \quad (51)$$

where $H = \sum_{k=i-1}^{i+1} \Delta x_k$ and $f = 0$ are taken as the bottom edge of the $(j-1)$ row of the cells.

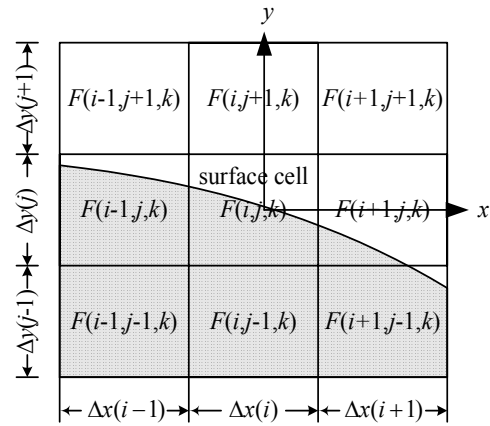


Fig. 9 Definition of cell block

The height difference dH in each-direction, as shown in Fig. 10 can be expressed as

$$dH = |m_\xi d\xi| + |m_\eta d\eta| \quad (52)$$

where $m_\xi = \partial f / \partial \xi$ and $m_\eta = \partial f / \partial \eta$.

Once the surface slope and the side occupied by fluid have been determined, a line can be constructed in the cell with the correct amount of fluid volume lying on the fluid side. This line is used as an approximation to the

actual surface and provides the information necessary to calculate the pressure interpolation factor ζ for the application of the free-surface pressure boundary conditions (Eq. 25).

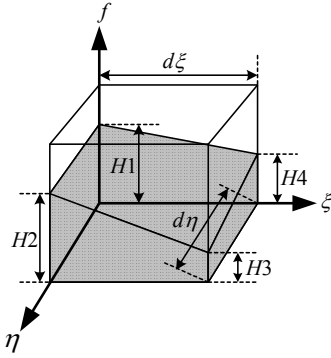


Fig. 10 Representation of height in a cell

(6) Mesh boundary conditions

At the mesh boundaries, several types of boundary conditions may be imposed using the layer of the fictitious cells that surround the mesh. The built-in types of boundary conditions are as follows: free-slip, no-slip, continuative and constant pressure boundary conditions. Consider a left boundary, for instance, as illustrated in Fig.11. If this is a rigid free-slip wall, then the normal velocity and the gradient of the tangential velocity are both set zero. Namely,

$$\begin{aligned} u_{1,j,k}^{n+1} &= 0; v_{1,j,k}^{n+1} = v_{2,j,k}^{n+1}; w_{1,j,k}^{n+1} = w_{2,j,k}^{n+1}; \\ F_{1,j,k}^{n+1} &= F_{2,j,k}^{n+1}; p_{1,j,k}^{n+1} = p_{2,j,k}^{n+1} \end{aligned} \quad (53a)$$

If the left boundary is a rigid no-slip wall, then both of the normal and tangential velocities are set to zero. That is to say,

$$\begin{aligned} u_{1,j,k}^{n+1} &= 0; v_{1,j,k}^{n+1} = -\frac{v_{2,j,k}^{n+1} \Delta x_1}{\Delta x_2}; \\ w_{1,j,k}^{n+1} &= -\frac{w_{2,j,k}^{n+1} \Delta x_1}{\Delta x_2}; F_{1,j,k}^{n+1} = F_{2,j,k}^{n+1}; p_{1,j,k}^{n+1} = p_{2,j,k}^{n+1} \end{aligned} \quad (53b)$$

For a continuative or outflow boundary, a prescription is needed so that the fluid may flow out of the domain computation. The continuative boundary conditions imposed at the left wall are expressed as

$$\begin{aligned} u_{1,j,k}^{n+1} &= u_{2,j,k}^{n+1}; v_{1,j,k}^{n+1} = v_{2,j,k}^{n+1}; w_{1,j,k}^{n+1} = w_{2,j,k}^{n+1}; \\ F_{1,j,k}^{n+1} &= F_{2,j,k}^{n+1}; p_{1,j,k}^{n+1} = p_{2,j,k}^{n+1} \end{aligned} \quad (53c)$$

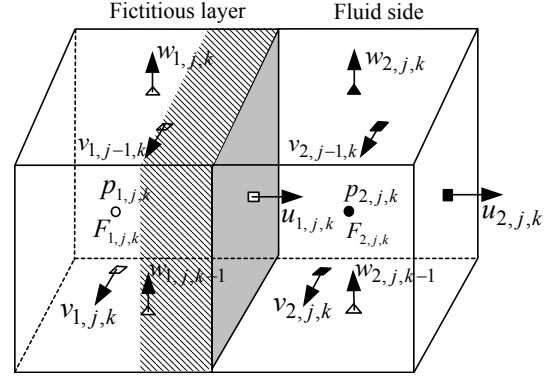


Fig. 11 Velocity boundary conditions near the left wall

(7) Numerical stability

Numerical calculations often have computed quantities that develop large high-frequency oscillations in space and time. This behavior is usually referred to as numerical instability, especially if the physical problem has unstable solutions and if the calculated results exhibit significant variations over distances comparable to a cell width or over times comparable to the time increment. If this happens, the accuracy of the calculated results cannot be relied on. To prevent such numerical instability or inaccuracy, certain restrictions should be observed in defining the mesh increments, the time increment and the upstream differencing parameter α .

The mesh increments should be chosen small enough to resolve the expected spatial variations in all dependent variables. Once a mesh has been chosen, the choice of the time increment necessary for stability is governed by two restrictions. First, fluid must not flow across more than one computational cell in one time step because the finite difference equations assume fluxes only between adjacent cells. Thus, the time increment must satisfy the following inequality

$$\Delta t_{CFL} < \min \left\{ \frac{C_r \Delta x}{|u|}, \frac{C_r \Delta y}{|v|}, \frac{C_r \Delta z}{|w|} \right\} \quad (54)$$

where the minimum is evaluated with respect to every cell in the mesh and C_r is a Courant number. Second, when a nonzero value of kinematic viscosity is used, the momentum must not diffuse more than approximately one cell in one time step. A linear stability analysis shows that this limitation implies

$$v \Delta t_{VIS} < \frac{1}{2} \frac{\Delta x^2 \Delta y^2 \Delta z^2}{(\Delta x^2 + \Delta y^2 + \Delta z^2)} \quad (55)$$

With Δt chosen to satisfy the above two inequalities, the last parameter needed to ensure numerical stability is

α . The proper choice for α is

$$1 \geq \alpha \max \left\{ \left| \frac{u\Delta t}{\Delta x} \right|, \left| \frac{v\Delta t}{\Delta y} \right|, \left| \frac{w\Delta t}{\Delta z} \right| \right\} \quad (56)$$

In the present computation code, the value of α is automatically adjusted to be:

$$\alpha = \min \left(1.2 \max \left\{ \left| \frac{u\Delta t}{\Delta x} \right|, \left| \frac{v\Delta t}{\Delta y} \right|, \left| \frac{w\Delta t}{\Delta z} \right| \right\}, 1 \right) \quad (57)$$

3. Simulation Results

3.1 Two-dimensional dam-break problem

We applied the proposed analysis procedure to a two-dimensional dam-break problem in which a column of water in air collapses under its own weight. This problem is selected because the initial flow configuration is simple and the experimental data are available. The computed results are compared with the experimental results by Martin and Moyce (1952).

The definition of the dam-break problem is illustrated in Fig. 12. The rectangular computational domain of size $5a \times a \times 1.5a$ is subdivided into a non-uniform mesh of 100 grids in the x -direction, 20 grids in the y -direction and 30 grids in the z -direction. The variables used in the computation are all non-dimensional variables by choosing a as reference length and $\sqrt{g_z a}$ as reference velocity. The non-dimensional viscous coefficient $\nu/[a\sqrt{(g_z a)}]$ is chosen at 10^{-5} and the non-dimensional time increment $\Delta T = \Delta t \sqrt{g_z/a}$ is taken as 0.005, where g_z is gravitational acceleration. In the problem under discussion a rectangular column of water is initially confined between a vertical wall and a gate and is in hydrostatic equilibrium. The water column is 1.0-unit wide and 1.0-unit high. Gravity is acting downward with unit magnitude. At the beginning of the calculation, the right wall (dam face) is removed and the reservoir dam water is allowed to flow out on to a dry horizontal floor.

It can be seen from Fig. 13 that the present analysis procedure captures the essential features of the free surface flow. The time histories of the water front location and water column height are shown in Fig. 14. The experimental results of Martin and Moyce (1952) with $a = 0.06$ m, $b = 0.06$ m and the calculated results in terms of two-dimensional LIQSEDFLOW (Sassa et. al., 2003) are also plotted in this figure. It is seen that the predicted performance compares favourably with the

observed flow behaviour, validating the three-dimensional analysis code developed.

The application of the 3D-analysis code truly three-dimensional flow problems is ongoing and will be published in the near future.

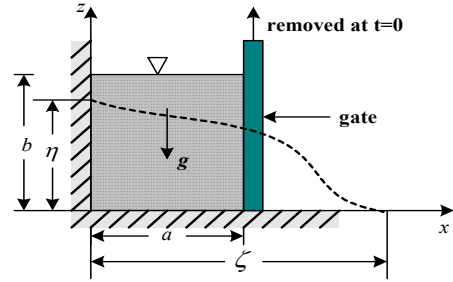


Fig. 12 Two-dimensional dam-break problem

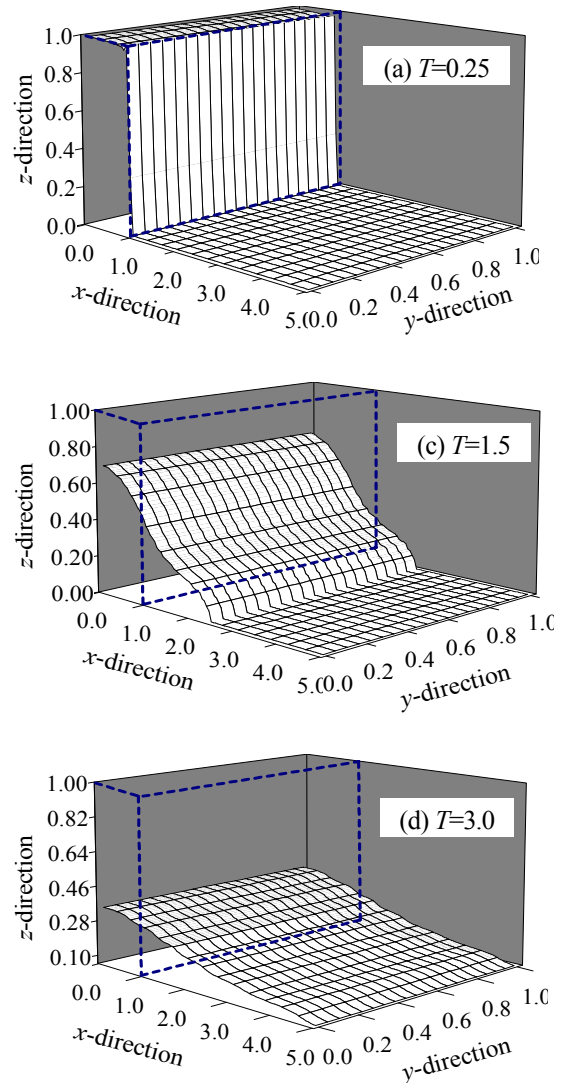


Fig. 13 Calculated fluid configurations in two-dimensional dam-break problem at three different times: (a) $T = 0.25$; (c) $T = 1.5$ and (c) $T = 3.0$ (..... represent initial fluid configuration)

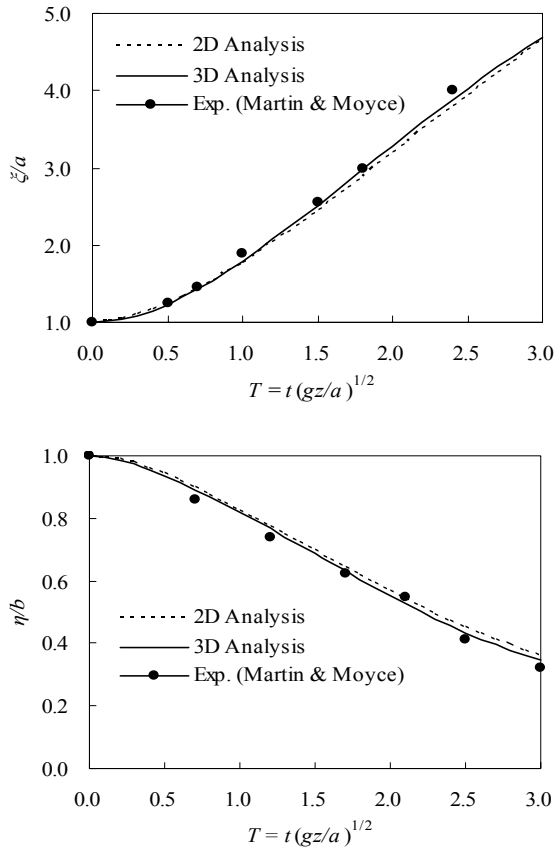


Fig. 14 Predicted and measured time histories of waterfront location and water column height in two-dimensional dam-break problem

3.2 Three-dimensional dam-break problem

The definition of the dam-break problem is illustrated in Fig. 15. The rectangular computational domain of size 5 x 1.2 x 1.5 is subdivided into a non-uniform mesh of 100 grids in the x -direction, 24 grids in the y -direction and 30 grids in the z -direction. A gate 0.3 m wide and 1.5 m high is provisioned in computational domain. For numerical conditions, the same condition as the two-dimensional dam-break problem is applied. In the problem under discussion a rectangular column of water is initially confined in a reservoir and is in hydrostatic equilibrium. At the beginning of the calculation, the gate is removed and the water is allowed to flow out on to a dry horizontal floor.

It is seen from Fig. 16 that the present analysis procedure captures the essential features of the three-dimensional free surface flow, warranting further scrutiny of the flow-out processes.

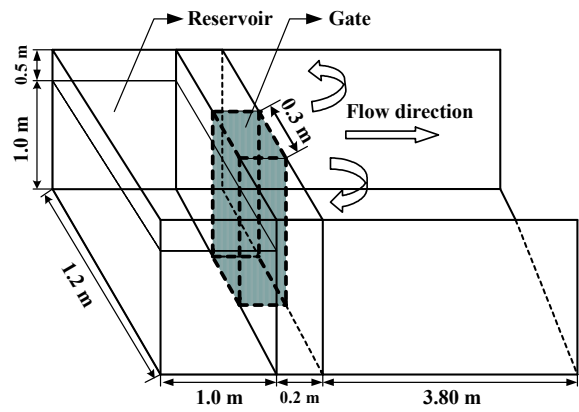


Fig. 15 Three-dimensional dam-break problem

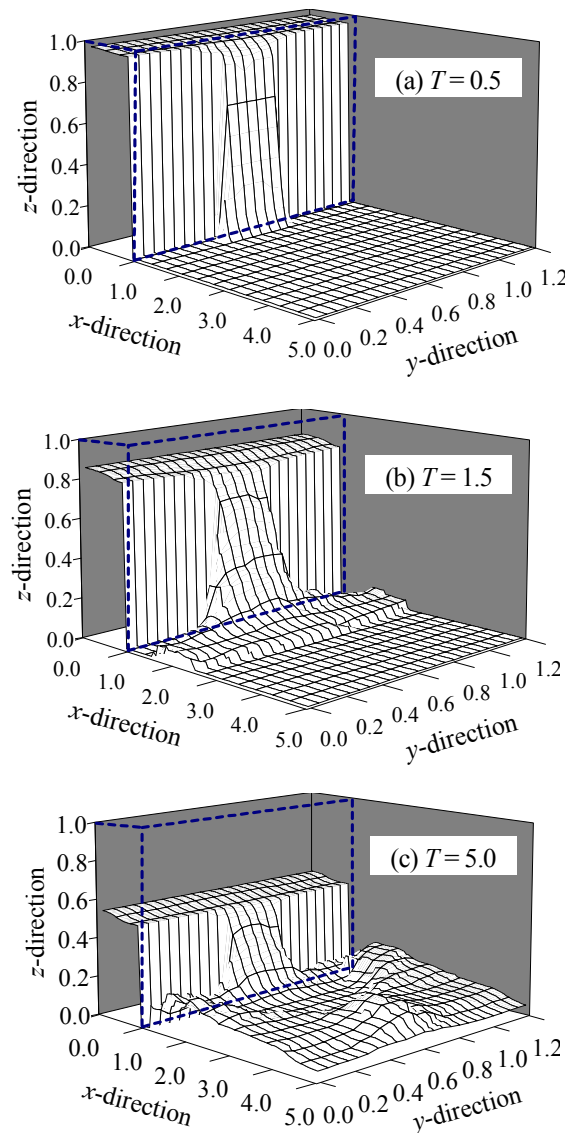


Fig. 16 Calculated fluid configurations in three-dimensional dam-break problem at three different times: (a) $T = 0.5$; (c) $T = 1.5$ and (c) $T = 5.0$ (..... represent initial fluid configuration)

4. Conclusions

A three-dimensional analysis procedure for describing the flow-out behaviour of liquefied soil with a free surface has been developed. The principal conclusions derived are as follows:

The predicted performance compares favourably with the results of two-dimensional experiments of Martin and Moyce (1952). The calculated results are also consistent with those predicted in terms of two-dimensional LIQSEDFLOW (Sassa et al., 2003).

A truly three-dimensional dam-break problem is worked out using the analysis code developed, inspiring a better physical perception.

It is a subject for future studies to consistently consider the effect of soil consolidation and other such sedimentary processes in a manner compatible with the present fluid-dynamics module. By doing so, it is hoped that the three-dimensional analysis procedure will find wider applications to sediment-related processes that operate in waterfronts and coastal oceans.

References

- Amsden, A.A. and Harlow, F.H. (1970): A simplified MAC technique for incompressible fluid flow calculations, *J. Comput. Phys.*, 6: pp. 322-325.
- Drago, M. (2002): A coupled debris flow-turbidity current model, *Ocean Engineering* 29: pp. 1769-1780
- Ferziger, J.H., and Peric, M. (1997): *Computational Methods for Fluid Dynamics*, Springer-Verlag.
- Hampton, M.A., Lee, H.J., and Locat J. (1996): Submarine landslides, *Reviews of Geophysics*, 34: pp. 33-60.
- Hamzah, M.A. (2001): Numerical simulations of tsunami pressure acting upon coastal barriers on wet and dry lands, Dr. Eng. Thesis, Kyoto University.
- Hirt, C. W. and Cook, J.L. (1972): Calculating three-dimensional flows around structures and over rough terrain, *J. Comput. Phys.*, 10: pp. 324-340.
- Hirt, C. W. and Nichols, B. D. (1981): Volume of fluid (VOF) method for the dynamics of free boundaries, *J. Comput. Phys.*, 39: pp. 201-225.
- Iverson, R.H. (1997): The physics of the debris flows, *Reviews of Geophysics*, 35: pp. 245-296.
- Kothe, D. B., Mjolsness, R. C., and Torrey, M. D. (1994): RIPPLE: A Computer Program for Incompressible Flows with Free Surfaces. Los Alamos Scientific Laboratory report LA-12007-MS.
- Lemos, C. M. (1991): Wave Breaking: A numerical study in *Lecturer Note in Engineering*, Edited by C. A. Brebbia and S. A. Orzag, Springer-Verlag.
- Martin, J. C. and Moyce, W.J. (1952): An experimental study of the collapse of liquid columns on a rigid horizontal plane, *Phil. Trans. Roy. Soc. London A*, Vol. 244, pp.312-324.
- Nichols, B. D. and Hirt, C. W. (1971): Improved free surface boundary conditions for numerical incompressible-flow calculations, *J. Comput. Phys.*, 8: pp. 434-448.
- Sassa, S., Miyamoto, J., Sekiguchi, H. (2003): The dynamics of liquefied sediment flow undergoing progressive solidification. In: *Submarine Mass Movements and Their consequences*, Kluwer Academic Publishers, pp. 95-102.
- Simpson, J.E. (1997): *Gravity Currents in the Environment and the Laboratory*, Second Edition, Cambridge University Press.

堆積物の重力流れの三次元解析

Amiruddin*・佐々真志**・関口秀雄

*京都大学大学院 土木工学科

**横須賀市長瀬 3-1-1 港湾空港技術研究所

要旨

沿岸域の未固結堆積土斜面において海底地すべりが発生すると、崩土は長距離にわたって沖合に流出することがある。実際、沿岸域と深海域を結ぶ重要な堆積物運搬作用として混濁流が知られているが、その物理機構には不明の点が多い。本研究は、堆積物の水中重力流れの発達、減速、停止の一連の過程を整合的に記述し得る解析コードの開発を行なったものである。液状化堆積物を高密度粘性流体と理想化し、自由表面を有する3次元重力流の解析コードを開発した。さらに、その予測能力を堆積物ダム決壊問題に照らして検討した。

キーワード： 液状化、三次元解析、堆積物重力流、ダム決壊問題